Sensors and Actuators Reports 3 (2021) 100027

Contents lists available at ScienceDirect

Sensors and Actuators Reports

journal homepage: www.elsevier.com/locate/snr

Ultra-sensitive wide-range small capacitive pressure sensor based on porous CCTO-PDMS membrane

Xingwei Tang [a], Qiao Gu [b], Ping Gao [b], Weijia Wen *,[a]

[a] Physics Department, The Hong Kong University of Science and Technology, Hong Kong
[b] Chemical and Biological Engineering Department, The Hong Kong University of Science and Technology, Hong Kong

ARTICLE INFO

Keywords:
Dielectric elastomer
Porous membrane
Capacitive pressure sensor
Ultra-sensitive

ABSTRACT

Dielectric elastomer is a very popular composite material used for different applications. Calcium copper titanate (CCTO) particles have a high dielectric constant, while polydimethylsiloxane (PDMS) is a commonly used flexible elastomer with good elastic property and durable chemical resistance, and their composite has shown an important and unique character for the fabrication of the pressure/force sensor. To improve the sensitivity of the capacitive sensor, various elastomers' microstructures have been introduced; but the methods used to manufacture microstructures in PDMS have so far been more difficult, requiring special equipment or hazardous chemicals such as strong acids and alkalis, otherwise, the sponge-like structures produced are slightly larger and cannot be applied to very small scenes. In this report, the extraction method was used to manufacture porous microstructures of the PDMS with multiple porosities; the influence of different porosities and pore sizes on the sensitivity of capacitive pressure sensors, which can increase the sensitivity of capacitive pressure sensors, the measuring force range, and also applied to tiny scenes, were explored. Additionally, the current methodology for manufacturing porous PDMS composite membranes is also suitable for the manufacture of other thinner PDMS composite porous membranes.

1. Introduction

The Capacitive Pressure Sensor is a measuring component that measures the force because the pressure affects the capacitance and causes the output power to change. Due to its simple structure [1,2], high temperature resistance [3,4], radiation resistance [5], high resolution [6], good dynamic response characteristics [7], etc., it is widely used in pressure [8,9], displacement [2,8], acceleration[10], thickness [3], vibration [5], liquid level [11] and other measurements [12]. It has also become an indispensable part of electronic wearable equipment [13,14] and various industrial automation environments (including water conservation [15] and hydropower [16], rail transit [17], and aerospace [18]). In view of the demand for micro-scale measurement, there is need for the manufacture of more sensitive sensors [19]. This led to the discovery that for capacitive pressure sensors, the dielectric constant and distance of electrode during compression are two very important factors [20], particularly after the size of the sensor have been determined. Hence, dielectric elastomer, a functional composite material which mixes high dielectric constant materials in an elastomer, has become highly desired because of its combination of high dielectric constant and good elasticity [21,22]. In addition, some microstructures and porous structures can help increase the greater change in distance during the pressing process with the same force, thereby improving the accuracy and measurement range of the capacitive pressure sensor [20,23,24].

Calcium copper titanate ($CaCu_3Ti_4O_{12}$, CCTO), a giant dielectric material and polydimethylsiloxane (PDMS), an elastomer, are widely used in dielectric elastomers [25–27] and they can be made into various dielectric elastomer actuators [28–30]. Since the CCTO hybrid PDMS improves the dielectric coefficient of the elastomer, the CCTO-PDMS composite plus the microstrutures can become an ultrasensitive capacitive sensor [31]. However, the spongy structure is relatively large, because the mold disappearance method (the mold is made into a built structure and then eroded) [31–33] is used to obtain this kind of structure. While trying to make miniature and small capacitive pressure sensors, the elastic body should not be too thick, and the limitation of the mold size makes the manufacture of the microstructures more difficult, which is not easy to achieve the adjustable pores' dimension. However, even if a mold of a suitable size is obtained, such as nano particles of a certain size, and then acid etching is used to remove them [34], the entire process is still wasteful and tedious. And the holes of the membrane made of the mold disappearance method all through. The porous CCTO-PDMS dielectric elastomer method obtained can fabricate a sufficiently thin membrane to make tiny holes, and the process is simple and easy to operate. The holes we get can be independent and non-through.

* Corresponding author.
E-mail address: phwen@ust.hk (W. Wen).

https://doi.org/10.1016/j.snr.2021.100027
Received 14 December 2020; Revised 12 January 2021; Accepted 17 January 2021
Available online 4 February 2021

For pure CCTO-PDMS medium [35], although its relative permittivity is high, its Young's modulus is also large, and it is not prone to deformation. Therefore, its sensitivity is not too high, and due to the characteristics of the elastomer, the force are exponentially related to the deformation. Therefore, even if it is a large force, the deformation will not change large, so it will easily reach the detection limit of the sensor. For sensors using CCTO/PDMS porous membrane [20], the Young's modulus of the composite material is reduced due to the addition of pores, and the deformation under the action of a small force is also large enough, so the sensitivity of the sensor is improved, and the sensitivity will change with the number and size of the holes. The addition of pores also increases the compressibility of the membrane and increases the detection range of the sensor. The previous method[31,32] of making porous membranes cannot easily produce thinner and adjustable pore sizes. Due to the fact that the elastomer is thin, it can be miniaturized and applied to finer scene measurement, and the method for making the porous membrane can also be applied to other scenes related to the production of composite PDMS porous membranes, giving new inspiration to the construction of microstructures such as for the fabrication of magnetic-based porous materials when the magnetic particles are added instead of CCTO. Porous elastomers also can be used for sound shielding purpose due to its porous character and elastic property.

2. Preparation and characterization of porous CCTO-PDMS membrane

2.1. Preparation of porous CCTO-PDMS membrane

Fig. 1 presents the method for making porous CCTO-PDMS membrane. First, the CCTO particles (Hunan Kelai New Material Co., Ltd.) are mixed with PDMS gel (Sylgard 184, Dow Corning) and mineral oil (Sonneborn). The size of the CCTO ranges from 3 to 5μm, while the weight ratio of the CCTO and PDMS gel is 20%. To prevent floating of the mineral oil and the uneven distribution of pores during the high temperature curing process, a 10:1.2 weight ration of the silicone elastomer base and the curing agentis used to accelerate the adhesion of PDMS gel. The amount of mineral oil is calculated according to the porosity of 10%, 20%, and 30% (the volume of mineral oil is the volume of all pores), respectively. Mixing and grinding using a high-energy ball mill (SPEX 8000M Mixer/Mill High-Energy Ball Mill) is done for one hour to uniform mixing, because it is found that the grinding time will not affect the pore size and shape. After ball milling, a uniform colloidal dispersion is obtained, and then a suitable heat setting method chosen for curing at 100°C depending on the shape and thickness of the desired film. Here, 40 μm thick membranes are made using the doctor blade method; 1 *mm* thick membranes are made by hot pressing. To ensure sufficient curing, since it is found that the strength of the elastomer will not change even if the temperature is maintained at 100°C after complete curing, the time for the curing process is kept at 1 h. After full curing, a CCTO-PDMS composite membrane with a uniform distribution of mineral oil beads is obtained. In order to obtain a porous structure, the composite membrane is immersed into hexane; the PDMS becomes swollen in hexane. PDMS is easily dissolved into Hexane due to the closed solubility parameters, even highly cross-linked PDMS can be swelled by Hexane with the maximum swell volume ratio around 2.7. And mineral oil is soluble in hexane, the fully swelled PDMS would have a loosely bonded interconnecting structure, so that the mineral oil can dissolve into the Hexane and gradually diffuse out by the concentration gradient, therefore forming pores in the CCTO-PDMS composite elastomer. Moreso, to ensure sufficient extraction, the composite membrane is soaked in hexane for 12 h (in fact, the extraction process is not so long); proper heating also speeds up the extraction process. The membrane from which the mineral oil has been extracted is collected awaiting volatilization of the hexane, then the preparation of the porous CCTO-PDMS membrane is complete.

2.2. Characterization of porous CCTO-PDMS membrane

The porous CCTO-PDMS membranes with different porosities (10%, 20%, and 30%) made are observed with SEM for their pore size and shape. Some shapes observed by SEM are shown in Fig. 2(a) and (b), while Fig. 2(a) presents observations for CCTO-PDMS porous membrane with a porosity of 30%. From observations, the pores in the porous membrane made by the extraction method are uniformly distributed in the body of the CCTO-PDMS membrane, not only on the surface of the membrane, and the pore sizes range from a few microns to tens of microns. For porous membranes with 10% (Fig. 2(b)) and 20% porosity, the pore size is much smaller than 30%, almost below ten microns. Comparing the cross-section and surface SEM of the porous membranes, it is observed that, these pores are not standard sphere. The dimension on the surface is bigger than the dimension on the cross-section, and the greater the porosity, the more obvious is the section. Therefore, we can conclude that the larger the porosity, the larger the pore size, and this size does not increase linearly. However, the size and shape of the pore has nothing to do with the grinding time with a ball mill, because from the SEM it is observed that the pore size did not change significantly with grinding time of 30, 45, or 90 mins. Through the XRD (Fig. 2(b) illustration) and elemental analysis (Fig. 2(c)) of the CCTO-PDMS porous membrane, it is found that the CCTO particles are very uniformly distributed in the PDMS, which shows a uniform dispersion system.

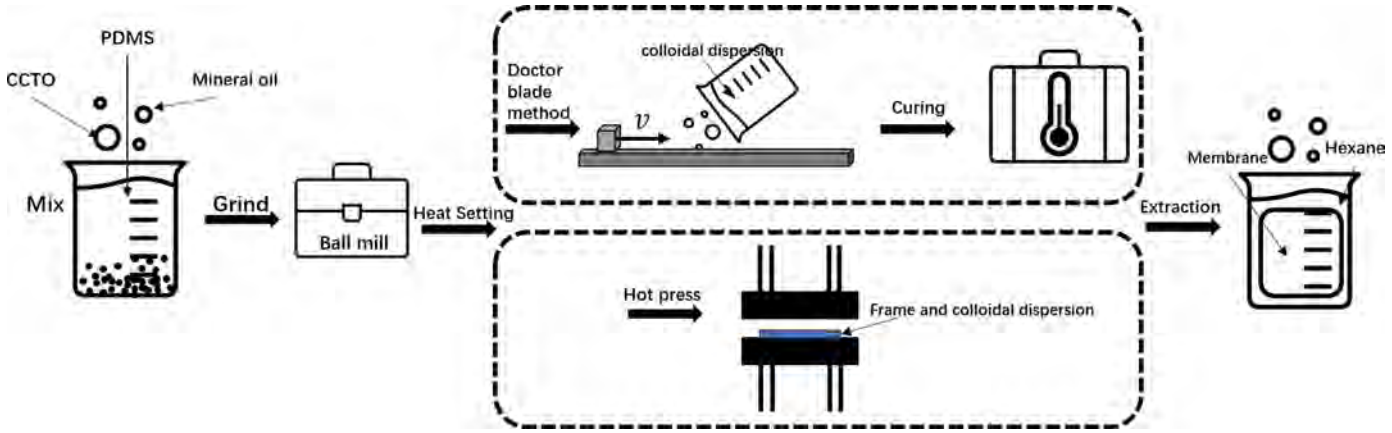

Fig. 1. Schematic diagram of the fabrication process for the porous CCTO-PDMS membranes: First, CCTO particles, PDMS gel, and mineral oil are evenly mixed using a ball mill. Then, a suitable heat setting process is chosen (doctor blade method or hot pressing method) according to the shape and thickness of the desired membrane. Finally, the cured membrane is placed into hexane and the mineral oil is extracted from it, this forms the porous CCTO-PDMS membrane.

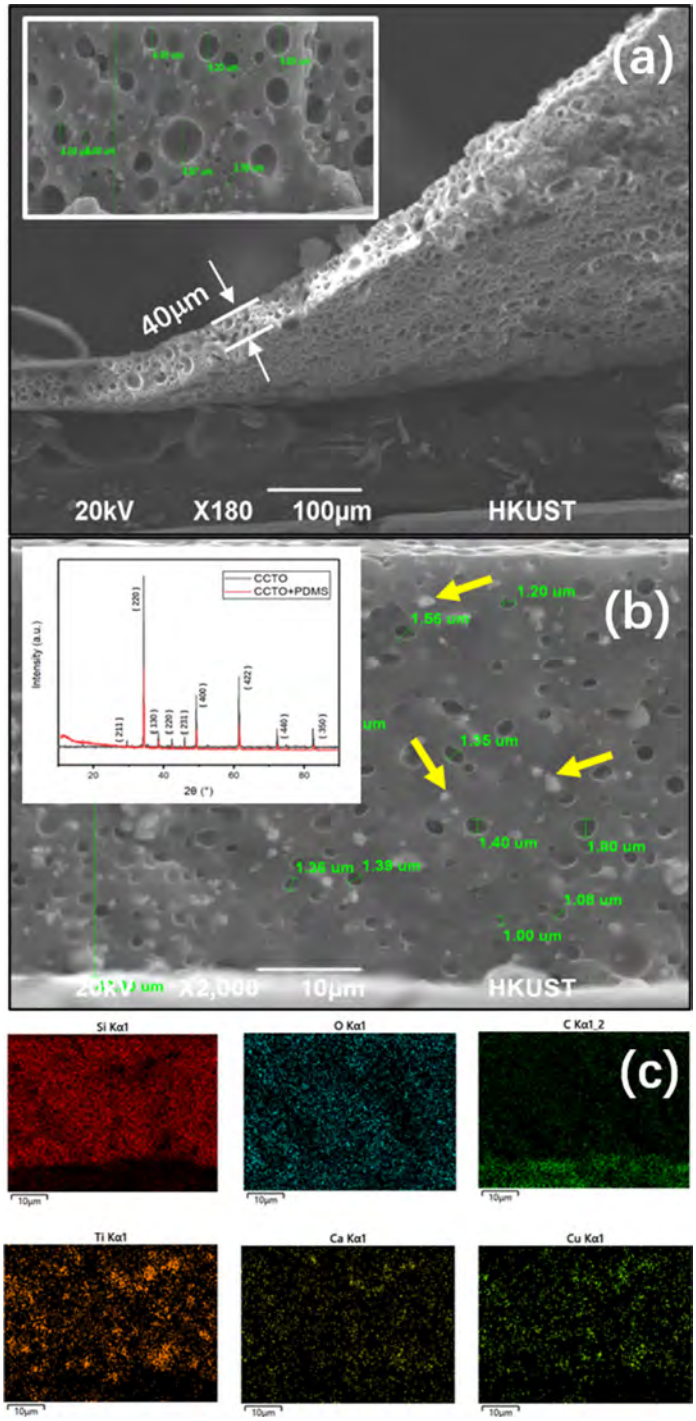

Fig. 2. (a) SEM of a CCTO-PDMS porous membrane with 30% porosity. The inset is a cross-sectional view of the porous membrane, including the pore size. (b) SEM of the cross-section of the CCTO-PDMS porous membrane with 10% porosity. The inset is the XRD of CCTO particles and CCTO-PDMS membrane. (c) Elemental analysis of the cross section of the CCTO-PDMS porous membrane.

In order to understand the influence of CCTO particles and microporous structure on the elastic modulus of PDMS, we used TA, ARES 3 to perform loop tensile test (Fig. 3(a)) and ultimate tensile test (Fig. 3(b)) similar to the illustration at the bottom of Fig. 3(b). It is observed that the addition of solid particles increases the Young's modulus of composite PDMS membrane, increases the stiffness, and weakens the ductility. However, the porous structure reduces the stiffness increased due to the addition of CCTO particles and also increases the ductility. Here, we build a model of a porous structure membrane and observed the effect of the porous structure. Although we already have the Gibson-Ashby formula to describe the porous structure, however, this model is a metal porous structure, which does not involve the effects of thermodynamics and air pressure [36], and it is believed that this model is not very consistent with our actual situation. Therefore, a model closer to our actual situation is built. Fig. 3(a) shows the schematic diagram of the model. The pores in the membrane are referred to as balls of radius R (although in reality our holes are not completely spherical, but all holes can be fitted with multiple balls, so in this case the spherical type is chosen). If the air pressure in the membrane is P_0 and the external atmospheric pressure is P_{PDMS}, the air pressure under stress in the membrane becomes $P_0^{'}$ and the external atmospheric pressure under stress becomes P, then the Laplace pressure is given as:

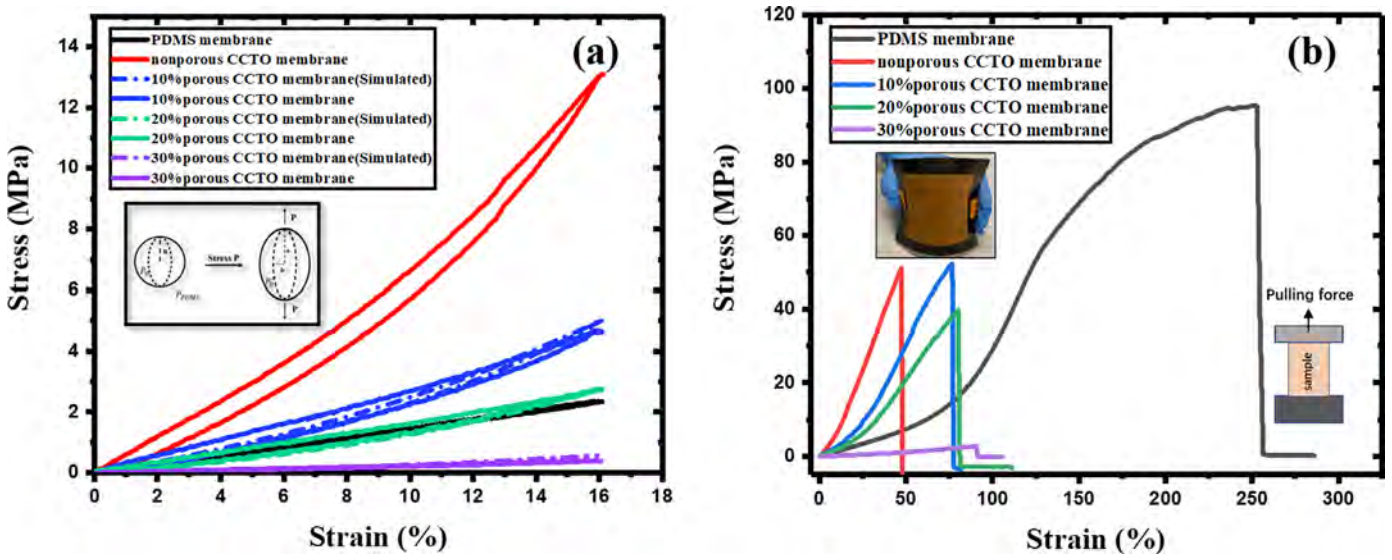

Fig. 3. (a) Loop tensile test of different membranes: strain-stress curves. The illustration shows the deformation of a spherical hole after stress. (b) Ultimate tensile test of different membranes: strain-stress curves. The upper illustration shows the softness of the CCTO-PDMS membrane, and the lower illustration shows the test method. All samples for tensile test are 10*mm* (length) × 5 mm (width) × 40 μm (thickness).

$$P_0 - P_{PDMS} = \frac{2\gamma}{R} \tag{1}$$

$$P_0^{'} + P - P_{PDMS} = \frac{2\gamma a}{b^2} \tag{2}$$

where R is the radius of the original sphere, γ is the surface tension of PDMS, a and b are the major and minor axes of the ellipsoidal hole due to stress. In order to minimize the overall energy of the bubble, the surface tension energy and gas energy need to be at their lowest:

$$\gamma \Delta S + P \Delta V = 0 \tag{3}$$

we take $\Delta V = 0$, the volume of spherical bubbles and ellipsoidal bubbles are the same, $4\pi R^3/3 = 4\pi ab^2/3$, so we obtain:

$$b^2 = \frac{R^3}{a}. \tag{4}$$

Combining Eq. (2), $\Delta V = 0$ and $P_0^{'} = P_0$, we obtain:

$$P = \frac{2\gamma}{R}(\eta^{'2} + 2\eta^{'}) = P_1(\eta^{'2} + 2\eta^{'}) \tag{5}$$

here, the strain is defined as: $\eta^{'} = (a - R)/R$, $P_1 = 2\gamma/R$, which means the difference between the internal and the external pressure in the original bubble. With the stress P, the total strain of the porous membrane becomes:

$$\eta_{tot} = (1 - V_{air})\eta + V_{air}\eta^{'} \tag{6}$$

hence, the stress P becomes:

$$P = \frac{k}{A}\eta_{tot} = \frac{k}{A}\left((1 - V_{air})\eta + V_{air}\eta^{'}\right) \tag{7}$$

here, k is the Young's modulus of nonporous membrane; A is the strain magnification of the V_{air} porous membrane. Combining Eq. (5), we obtain:

$$\eta^{'} = \frac{1}{2P_1}\left(-\left(2P_1 - \frac{k}{A}V_{air}\right) + \left(\left(2P_1 - \frac{k}{A}V_{air}\right)^2 + 4P_1\frac{k}{A}\left((1 - V_{air})\eta\right)^{1/2}\right)\right). \tag{8}$$

The strain magnification A of the V_{air} porous membrane is given as:

$$A = \frac{V_{air}\sqrt{P_1(P_1 + k\eta)} - P_1(V_{air} - \eta + V_{air}\eta)}{P_1\eta}. \tag{9}$$

By applying the constructed model to our actual situation, and using the experimental result of the loop tensile test of the nonporous CCTO-PDMS membrane, and the average radius of 10%(4 μm), 20%(5 μm), and 30% porosity(15 μm), the simulation result shown in Fig. 3(a) represented with dashed lines is obtained, which fits very well with the actual tensile loop test.

3. Ultra-sensitive wide-range small capacitive pressure sensor

According to the analysis of the strain-stress curves of different membranes, we believe that although the introduction of CCTO particles into the PDMS increases the Young's modulus, the high dielectric coefficient of the CCTO particles is still coveted as a sensitive capacitive sensor, thus the porous microstructure is introduced to improve the flexibility of the CCTO-PDMS membrane, so that it has a greater depression depth under the same pressing pressure, and increased the amount of capacitance change. Therefore, different CCTO-PDMS membranes (both 1 mm in thickness) are used as the medium of the membrane capacitors with the same plate (4.9 cm × 4.9 cm), and then the same force is applied on the same area (a circle with a diameter of 11.25 mm) and the same position of the membrane capacitors. The sensitivity is determined by the amount of capacitance change. Capacitance change detection circuit is based on the resonance mechanism and consists of four parts, as shown in Fig. 4(a). For the *RLC* resonance circuit, the voltage amplitude Y on the inductor is given by:

$$|Y| = \frac{Y_m}{\left[1 + \left(wL - \frac{1}{wC}\right)^2/R^2\right]^{1/2}} \tag{10}$$

where w is the angular frequency set as 130 kHz, Y_m denotes the maximum amplitude of Y, and our input voltage for the detection circuit is 300 mV. When applying the force to the membrane capacitor, due to the different dielectric coefficients and the different stress and strain of different membranes, the change in the different membrane capacitors capacitances also vary, $C(F) = \frac{\varepsilon_0\varepsilon_r S}{d_0 - d(F)}$, and F is the pressing force. The sensitivity S of the voltage change caused by the membrane capacitance change in this circuit is defined as:

$$S = \frac{Y(C + \Delta C) - Y(C)}{Y(C)}. \tag{11}$$

Fig. 4 (b) show the different voltage amplitudes output by different membrane capacitors and the real-time measurement is done by the

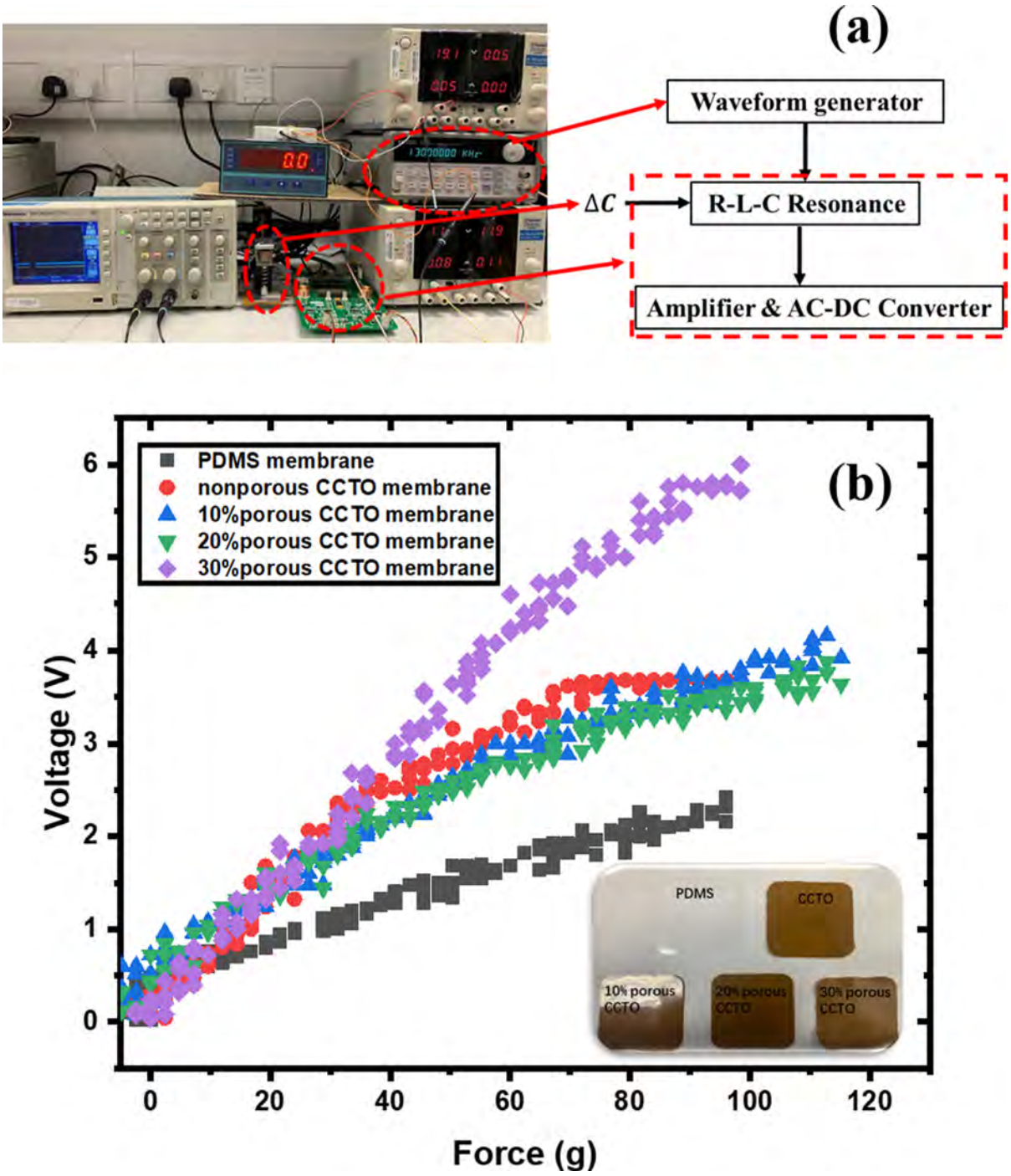

Fig. 4. (a) Experimental setup: an *AC* waveform generator that can output waveform with adjustable amplitude and frequency; an *RLC* resonance circuit where the capacitor *C* comes from the membrane capacitance; an amplifier and an $AC-DC$ converter that output voltage corresponding with the variable membrane capacitance. (b) The voltage change of different membrane capacitances under different pressing forces. The illustrations are images of different membranes.

oscilloscope. In the video in the supplementary material, the real-time rapid voltage change due to the force can also been seen. According to the result in Fig. 4(b), the non-porous CCTO-PDMS membrane doubles the sensitivity of the PDMS membrane. And the sensitivity of the 10% porous CCTO-PDMS membrane and the 20% porous CCTO-PDMS membrane seemed similar to the non-porous CCTO-PDMS membrane (although the more the holes, the smaller the rigidity, but it also reduces the dielectric coefficient of the composite material, and in this case, the changes of the rigidity and the dielectric coefficient just cancel each other), however, the non-porous CCTO-PDMS membrane reaches the range when the force is $75g$, and according to Fig. 3(b), more holes and larger holes will effectively increase the range due to the increase in ductility and the decrease in rigidity. Therefore, the sensitivity of the 30% porous CCTO-PDMS membrane is twice that of the PDMS membrane and 0.5 times that of the non-porous CCTO-PDMS membrane, and the effective range is also greatly improved. According to the determining formula of the capacitance, the membrane capacitance is determined by the dielectric coefficient, the area of the plate and the thickness of the membrane. According to the definition of sensitivity, Eq. (11), the greater the ΔC, the better the sensitivity of the membrane capacitor (Fig. 5(a)). In the initial situation, all membrane capacitors only have different dielectric coefficients. The more the pores, the more the air is

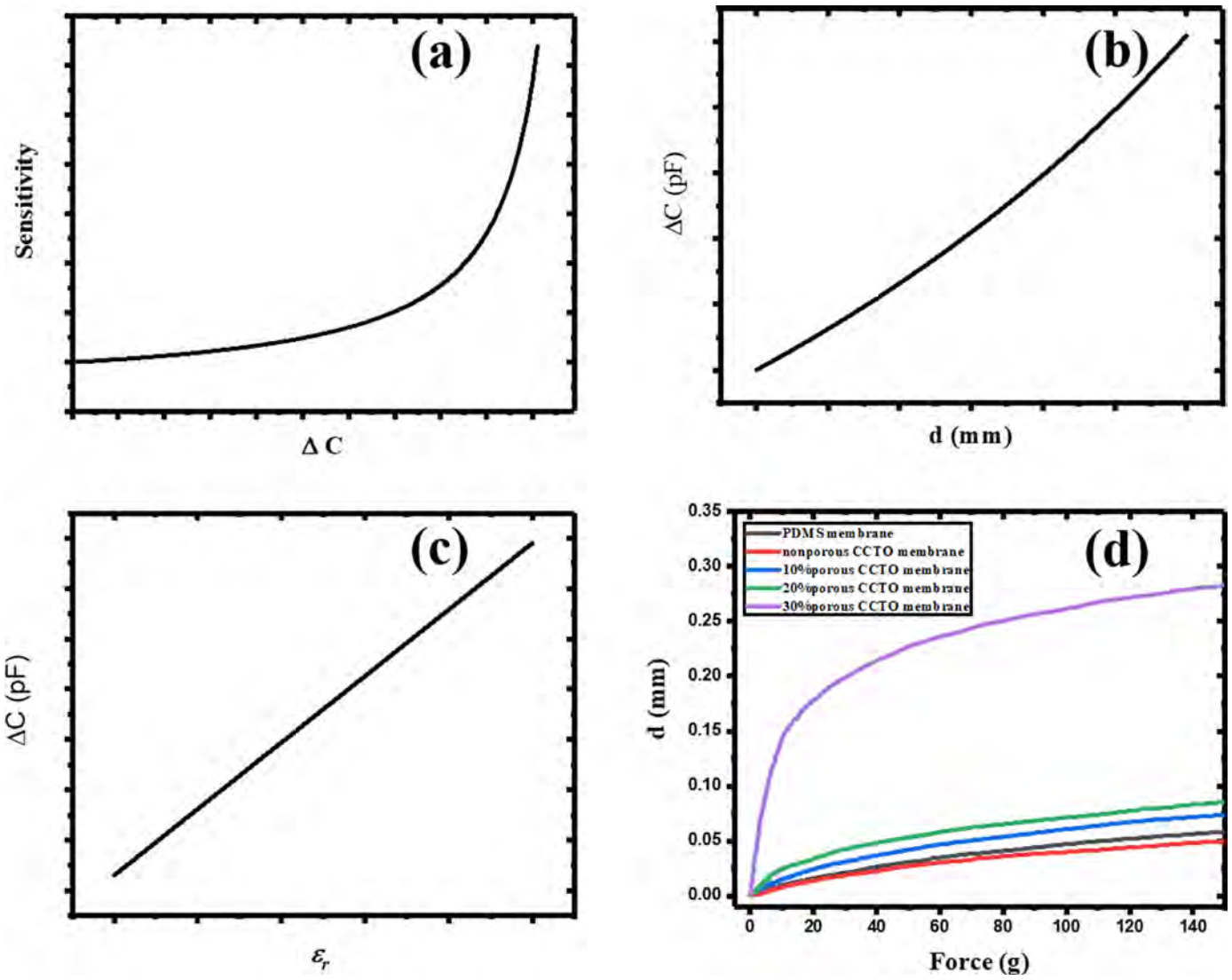

Fig. 5. (a) The relationship between voltage sensitivity and ΔC under the same applied force. (b) The relationship between depression depth and ΔC. (c) The relationship between relative permittivity and ΔC under the same depression depths. (d) The relationship between the force on different membranes and the depth of depression.

connected in parallel with CCTO-PDMS, and the relative permittivity will decrease. Then through the determining formula of the capacitance, we found that the larger the relative dielectric coefficient, the larger the ΔC (as shown in Fig. 5(c)), which increase the sensitivity of the sensor. However, with the application of the same force, different membranes have different depression depths with different proportions of materials (as shown in Fig. 5(d)), and the larger the d, the larger the ΔC (as shown in Fig. 5(b)). Therefore, the dielectric coefficient of the CCTO membrane is greater than that of PDMS and the capacitance properties of the CCTO membrane are better than those of PDMS. The porous CCTO membrane contain pores, and the larger the pore size, the smaller the dielectric coefficient, but the pore size also cause greater pressing depth. When the pore size reaches a certain level, it can offset the disadvantage of low dielectric coefficient, also when the pore size is large, it can show better sensitivity than the high dielectric coefficient membranes. Because of the porous structure, the depth that can be pressed is greater, and the measuring force range is increased accordingly.

4. Conclusion

In summary, the porous CCTO-PDMS membrane can act as an ultra-sensitive wide-range small capacitive pressure sensor, and a porous structure with certain porosity can compensate for the decrease in relative permittivity. The extraction method for preparing porous CCTO-PDMS membrane leads to the preparation of a porous microstructure. The entire preparation process is simple and provides a new idea for other composite PDMS porous films.

Declaration of Competing Interest

The authors declare no conflict of interest.

Acknowledgments

Tang X.W. would like to thank Mr. Qianhang Ding for the useful discussions. The authors would like to acknowledge the support of the technicians and researchers from Design and Manufacturing Services Facility (DMSF) at the Hong Kong University of Science and Technology. The work is supported by an Hong Kong Areas of Excellence Scheme grant (AOE/P-02/12) and HK RGC 16204019.

Supplementary material

Supplementary material associated with this article can be found in the online version at doi: 10.1016/j.snr.2021.100027

References

[1] J. Wang, R. Suzuki, M. Shao, F. Gillot, S. Shiratori, Capacitive pressure sensor with wide-range, bendable, and high sensitivity based on the bionic Komochi Konbu structure and Cu/Ni nanofiber network, ACS Appl. Mater. Interfaces 11 (12) (2019) 11928–11935.

[2] M.-X. Zhou, Q.-A. Huang, M. Qin, W. Zhou, A novel capacitive pressure sensor based on sandwich structures, J. Microelectromech. Syst. 14 (6) (2005) 1272–1282.

[3] D.J. Young, J. Du, C.A. Zorman, W.H. Ko, High-temperature single-crystal 3c-sic capacitive pressure sensor, IEEE Sens. J. 4 (4) (2004) 464–470.

[4] Y.S. Lee, K.D. Wise, A batch-fabricated silicon capacitive pressure transducer with low temperature sensitivity, IEEE Trans. Electron Dev. 29 (1) (1982) 42–48.

[5] T.B. Gabrielson, Mechanical-thermal noise in micromachined acoustic and vibration sensors, IEEE Trans. Electron Dev. 40 (5) (1993) 903–909.

[6] Z. He, W. Chen, B. Liang, C. Liu, L. Yang, D. Lu, Z. Mo, H. Zhu, Z. Tang, X. Gui, Capacitive pressure sensor with high sensitivity and fast response to dynamic interaction based on graphene and porous nylon networks, ACS Appl. Mater. Interfaces 10 (15) (2018) 12816–12823.

[7] S. Wan, H. Bi, Y. Zhou, X. Xie, S. Su, K. Yin, L. Sun, Graphene oxide as high-performance dielectric materials for capacitive pressure sensors, Carbon 114 (2017) 209–216.

[8] K.F. Lei, K.-F. Lee, M.-Y. Lee, Development of a flexible PDMS capacitive pressure sensor for plantar pressure measurement, Microelectron. Eng. 99 (2012) 1–5.

[9] L. Chen, M. Mehregany, A silicon carbide capacitive pressure sensor for in-cylinder pressure measurement, Sens. Actuators A 145 (2008) 2–8.

[10] W.H. Ko, Q. Wang, Touch mode capacitive pressure sensors for industrial applications, in: Proceedings IEEE The Tenth Annual International Workshop on Micro Electro Mechanical Systems. An Investigation of Micro Structures, Sensors, Actuators, Machines and Robots, IEEE, 1997, pp. 284–289.

[11] F. Reverter, X. Li, G.C. Meijer, Liquid-level measurement system based on a remote grounded capacitive sensor, Sens. Actuators A 138 (1) (2007) 1–8.

[12] Y. Zhang, R. Howver, B. Gogoi, N. Yazdi, A high-sensitive ultra-thin mems capacitive pressure sensor, 2011 16th International Solid-State Sensors, Actuators and Microsystems Conference, IEEE, 2011, pp. 112–115.

[13] B. Ji, Q. Zhou, G. Chen, Z. Dai, S. Li, Y. Xu, Y. Gao, W. Wen, B. Zhou, In situ assembly of a wearable capacitive sensor with a spine-shaped dielectric for shear-pressure monitoring, J. Mater. Chem. C (2020).

[14] A. Pantelopoulos, N.G. Bourbakis, A survey on wearable sensor-based systems for health monitoring and prognosis, IEEE Trans. Syst. Man Cybern. Part C 40 (1) (2009) 1–12.

[15] H. Yin-Sung, C.-M. Wei, T. Yuan-Chi, Y. Shih-Yi, C.-L. Chang, K.-C. Chang, Capacitive sensing technique for silt suspended sediment concentration monitoring, Int. J. Sediment Res. 25 (2) (2010) 175–184.

[16] D. Jiang, M. Xu, M. Dong, F. Guo, X. Liu, G. Chen, Z.L. Wang, Water-solid triboelectric nanogenerators: an alternative means for harvesting hydropower, Renew. Sustain. Energy Rev. 115 (2019) 109366.

[17] J. Feng, J. Xu, W. Liao, Y. Liu, Review on the traction system sensor technology of a rail transit train, Sensors 17 (6) (2017) 1356.

[18] D.G. Senesky, B. Jamshidi, K.B. Cheng, A.P. Pisano, Harsh environment silicon carbide sensors for health and performance monitoring of aerospace systems: a review, IEEE Sens. J. 9 (11) (2009) 1472–1478.

[19] S.A. Wilson, R.P. Jourdain, Q. Zhang, R.A. Dorey, C.R. Bowen, M. Willander, Q.U. Wahab, S.M. Al-hilli, O. Nur, E. Quandt, et al., New materials for micro-scale sensors and actuators: an engineering review, Mater. Sci. Eng. 56 (1–6) (2007) 1–129.

[20] R. Li, Q. Zhou, Y. Bi, S. Cao, X. Xia, A. Yang, S. Li, X. Xiao, Research progress of flexible capacitive pressure sensor for sensitivity enhancement approaches, Sens. Actuators A (2020) 112425.

[21] F. Carpi, S. Bauer, D. De Rossi, Stretching dielectric elastomer performance, Science 330 (6012) (2010) 1759–1761.

[22] M. Wissler, E. Mazza, Mechanical behavior of an acrylic elastomer used in dielectric elastomer actuators, Sens. Actuators A 134 (2) (2007) 494–504.

[23] B. Ji, Q. Zhou, J. Wu, Y. Gao, W. Wen, B. Zhou, Synergistic optimization towards the sensitivity and linearity of flexible pressure sensor via double conductive layer and porous micro-dome array, ACS Appl. Mater. Interfaces (2020).

[24] L. Pan, A. Chortos, G. Yu, Y. Wang, S. Isaacson, R. Allen, Y. Shi, R. Dauskardt, Z. Bao, An ultra-sensitive resistive pressure sensor based on hollow-sphere microstructure induced elasticity in conducting polymer film, Nat. Commun. 5 (1) (2014) 1–8.

[25] Y.-Y. Zhang, Y. Min, G.-L. Wang, Z.-F. Wang, J.-L. Liu, Z.-W. Luo, M. Zhang, Design and properties of calcium copper titanate/poly (dimethyl siloxane) dielectric elastomer composites, Rare Met. (2019) 1–6.

[26] F.B. Madsen, A.E. Daugaard, S. Hvilsted, A.L. Skov, The current state of silicone-based dielectric elastomer transducers, Macromol. Rapid Commun. 37 (5) (2016) 378–413.

[27] G.L. Wang, Y.Y. Zhang, L. Duan, K.H. Ding, Z.F. Wang, M. Zhang, Property reinforcement of silicone dielectric elastomers filled with self-prepared calcium copper titanate particles, J. Appl. Polym. Sci. 132 (39) (2015).

[28] Y.Y. Zhang, G.L. Wang, J. Zhang, K.H. Ding, Z.F. Wang, M. Zhang, Preparation and properties of core-shell structured calcium copper titanate@ polyaniline/silicone dielectric elastomer actuators, Polym. Compos. 40 (S1) (2019) E62–E68.

[29] L.J. Romasanta, M.A. López-Manchado, R. Verdejo, Increasing the performance of dielectric elastomer actuators: a review from the materials perspective, Prog. Polym. Sci. 51 (2015) 188–211.

[30] L.J. Romasanta, P. Leret, L. Casaban, M. Hernández, A. Miguel, J.F. Fernández, J.M. Kenny, M.A. Lopez-Manchado, R. Verdejo, Towards materials with enhanced electro-mechanical response: Cacu 3 ti 4 o 12−polydimethylsiloxane composites, J. Mater. Chem. 22 (47) (2012) 24705–24712.

[31] C. Mu, J. Li, Y. Song, W. Huang, A. Ran, K. Deng, J. Huang, W. Xie, R. Sun, H. Zhang, Enhanced piezocapacitive effect in cacu3ti4o12−polydimethylsiloxane composited sponge for ultrasensitive flexible capacitive sensor, ACS Appl. Nano Mater. 1 (1) (2017) 274–283.

[32] A. Chhetry, S. Sharma, H. Yoon, S. Ko, J.Y. Park, Enhanced sensitivity of capacitive pressure and strain sensor based on CaCu3Ti4O12 wrapped hybrid sponge for wearable applications, Adv. Funct. Mater. (2020) 1910020.

[33] S. Wu, J. Zhang, R.B. Ladani, A.R. Ravindran, A.P. Mouritz, A.J. Kinloch, C.H. Wang, Novel electrically conductive porous PDMS/carbon nanofiber composites for deformable strain sensors and conductors, ACS Appl. Mater. Interfaces 9 (16) (2017) 14207–14215.

[34] X. He, X. Mu, Q. Wen, Z. Wen, J. Yang, C. Hu, H. Shi, Flexible and transparent triboelectric nanogenerator based on high performance well-ordered porous PDMS dielectric film, Nano Res. 9 (12) (2016) 3714–3724.

[35] J. Kim, H. Ryu, J.H. Lee, U. Khan, S.S. Kwak, H.-J. Yoon, S.-W. Kim, High permittivity CaCu3Ti4O12 particle-induced internal polarization amplification for high performance triboelectric nanogenerators, Adv. Energy Mater. 10 (9) (2020) 1903524.

[36] L.J. Gibson, M.F. Ashby, Cellular Solids: Structure and Properties, Cambridge university press, 1999.